Submitted to the IInd Aix-en-Provence
Conference on Elementary Particles
September 6-12, 1973

CERN/D.Ph.II/PHYS 73-29
9.8.1973

PRISM PLOT ANALYSIS OF THE FOUR-BODY REACTION

$\pi^- p \to p\pi^+\pi^-\pi^-$ AT 3.93 GeV/c

A. FERRANDO, V. CHALOUPKA, M. LOSTY, L. MONTANET
E. PAUL, D. YAFFE, A. ZIEMINSKI
CERN

ABSTRACT

We present an analysis of 20 000 events corresponding to the four-body reaction $\pi^- p \to p\pi^+\pi^-\pi^-$ at 3.93 GeV/c, using a complete set of seven variables necessary to specify such a reaction. The choice of the variables and the method adopted are those of the "MIT prism plot analysis". The distribution of the events over the competing channels is determined and the residual contamination are estimated. In addition the analysing power of the prism plot method is studied in more detail for two "well known" channels : $p A_2^-$ and $\Delta^0\rho^0$.

LM/mk

1. INTRODUCTION

The prism plot analysis is an iterative procedure proposed by J.A. Pless and collaborators [1], with the aim of separating the intermediate channels contributing to a given n-particle final state, using a complete set of (3n-5) variables needed to describe the process, excluding spin variables. The method is based on the idea that the use of a complete set of variables would reduce the overlaps between different competing channels. The choice of the variables is flexible. In this analysis we shall follow ref. [1], e.g., we shall use three kinetic energies, three longitudinal phase space variables and as a seventh variable the modulus of the transverse momentum of the $\pi^-\pi^-$-system. This choice is known to be useful at high energies when separating channels by studying projections out of the full phase-space.

The method neglects interference effects between the intermediate channels although they are probably playing an inportant role at this low energy. (It is in principle possible to incorporate them by assuming some model, but it complicates very much the analysis of this four-body reaction).

Technical details on the prism plot analysis and some results are already reported elsewhere [1].

In the following we underline the limitation of this method in its present form and discuss two specific tests made on the spin-parity of the $\pi^+\pi^-\pi^-$-system for the p A_2^- - channel and on the production mechanism of the $\Delta^0\rho^0$ - channel, respectively.

2. ANALYSIS AND GENERAL RESULTS

The data input to this analysis consists of 19442 events corresponding to the reaction

$$\pi^- p \to p\pi^+\pi^-\pi^- \quad \text{at 3.93 GeV/c}$$

obtained from the measurement of four-prong events observed in an exposure

of the CERN 2m hydrogen bubble chamber. The events were measured on the CERN spiral reader (LSD). This sample of events is relatively free of kinematical biases (we have checked that events not successfully measured do not correspond to a special configuration), and the separation of this 4c fit final state from others is better than 98%. The mass resolution is about ± 6 MeV for the $\pi^+\pi^-$ effective mass in the ρ region. The precision is sufficient for the analysis of the properties of the broad resonances in which we shall be mainly interested in the following. More details on data collection and the measurements can be found in ref. [2].

Figure 1 shows the two-and three-body effective mass distribution. Figure 1a shows the $\pi^+\pi^-$ mass with a large ρ^o - signal and a small shoulder at the position of the f^o. In fig. 1b one sees the $p\pi^+$ mass with the copious production of Δ^{++}, and in fig. 1c the three isobar objects $\Delta^o(1234)$, $N^{*o}(1520)$ and $N^{*o}(1680)$ above a rather large background Figure 1d displays the $\pi^+\pi^-\pi^-$ mass spectrum. A_2^- is clearly seen and the excess of events around 1.1 GeV could be attributed to some A_1^- production. The $p\pi^+\pi^-$ mass distribution (fig. 1e) indicates some N^* production or some diffraction dissociation effect in the low mass region.

We are then led to introduce the following channels which will be assumed to be incoherent :

(1) $\pi^- p \to p\, A_1^-$, $A_1^- \to \rho^o\pi^-$, $\rho^o \to \pi^+\pi^-$

(2) $\pi^- p \to p\, A_2^-$, $A_2^- \to \rho^o\pi^-$, $\rho^o \to \pi^+\pi^-$

(3) $\pi^- p \to N^{*o}(1520)\rho^o$, $N^{*o}(1520) \to p\pi^-$, $\rho^o \to \pi^+\pi^-$

(4) $\pi^- p \to N^{*o}(1688)\rho^o$, $N^{*o}(1688) \to p\pi^-$, $\rho^o \to \pi^+\pi^-$

(5) $\pi^- p \to \Delta^o(1236)\rho^o$, $\Delta^o(1236) \to p\pi^-$, $\rho^o \to \pi^+\pi^-$

(6) $\pi^- p \to \Delta^{++}(1236)\pi^-\pi^-$, $\Delta^{++}(1236) \to p\pi^+$

(7) $\pi^- p \to (DD)\pi^-$, $(DD) \to \Delta^{++}\pi^-$, $\Delta^{++} \to p\pi^+$

(8) $\pi^- p \to (DD)\pi^-$, $(DD) \to p\pi^+\pi^-$

(9) $\pi^- p \to p\pi^- f^o$, $f^o \to \pi^+\pi^-$

(10) $\pi^- p \to p\pi^+\pi^-\pi^-$ (phase space)

Masses and widths of the resonances are given in table 1. (DD) means diffraction dissociation of the target; the $p\pi^+\pi^-$ mass spectrum assumed for this process is also indicated in table 1.

Table 2 gives an explicit definition of the variables we used and their range. For the prism plot analysis one has to define a box as an element of the seven-dimensional space. We have used for each iteration step four box sizes corresponding to $\frac{1}{40}$, $\frac{1}{30}$, $\frac{1}{20}$ and $\frac{1}{10}$ of the range of each of the seven variables, respectively.

The number of events and corresponding percentages assigned by the prism plot analysis to each of the ten channels, after 13 iterations are given in the first part of table 3. These percentages were found to be stable after the tenth iteration. One notices the small fraction attributed to phase space.

Figures 2, 3 and 4 show some distributions obtained from the separated channels. A_1^- and A_2^- show up with the expected masses and widths (figs. 2a and b). The $\pi^+\pi^-$ mass distribution for the $p\,A_2^-$ channel (fig. 2c) shows the ρ^o signal induced by the A_2^- decay. Figures 2d and 2e display the $p\pi^-$ mass spectrum of $\Delta^o(1236)$ and the $\pi^+\pi^-$ mass spectrum of the associated ρ^o for the $\Delta^o\rho^o$ channel. The Δ^{++}-signal of the $\Delta^{++}\pi^-\pi^-$-channel can be seen in fig. 2f, and the $\pi^-\pi^-$ mass spectrum of the same events in fig. 2g. Figure 2h shows the $(p\pi^+\pi^-)$ mass spectrum attributed to the $(DD)\pi^-$-channel (number 8); it exhibits three-body N^* resonances.

The production angular distributions (fig. 3a to 3f) are consistent with the expected peripherality.

In fig. 4 we display some of the mass spectra which should not show resonance production after the selection operated by the prism plot analysis. One clearly observes several "wrong" signals like the Δ^{++} in the $\Delta^o\rho^o$ channel (fig. 4d). Using these distributions, and several similar ones, we can estimate the residual contaminations and their origin, for each"separated"channel. These estimations are given in table 3.

A more detailed analysis of this "overlap" between the different channels, making use in particular of events generated by Monte-Carlo techniques, can be found in ref. [4].

Table 3 shows that the p A_1^- - channel still contains a large contamination of N^{*0} and Δ^{++}. This is not the case for the p A_2^- - channel which appears to be better separated than most of the other channels. The $\Delta^0\rho^0$ - channel contains a large contamination of Δ^{++} ($\sim$ 10%). Moreover it is probably unreasonable to expect a complete separation of closely related channels like p A_1^- and p A_2^-, or $N^{*0}(1520)\rho^0$ and $N^{*0}(1688)\rho^0$, respectively.

We shall discuss now in more details the properties of the p A_2^- and the $\Delta^0\rho^0$ channels.

3. SPIN-PARITY OF THE $(\pi^+\pi^-\pi^-)$ - SYSTEM IN THE A_2 REGION.

We first combine the events which have been labelled p A_1^- or p A_2^- by the prism plot analysis, and then, following the method of Abramovich et al [5], we perform a spin-parity analysis for the 3π system which satisfy the condition: $1.30 \leq M(3\pi) \leq 1.34$ GeV. We apply the same spin-parity analysis to the other eight channels in order to estimate losses of the A_2^- signal into these channels. Finally, the same analysis is applied to the unseparated sample of events, the result being used as a reference for the total A_2^- signal.

Table 4 gives the number of events attributed to the usual set of spin-parity assignments, for the whole data and for each separated channel. Identifying the A_2^- signal with the 2^+ contribution, we can see that 73% of the A_2^- contained in the total sample are correctly attributed to p A_2^- by the prism plot analysis. The remaining 27% of A_2^- are spread over the other channels, mainly over those channels producing ρ^0. In fact, if we anti select the non-ρ^0- producing channels we get a result in good agreement with the full 2^+ contribution (see table 4). On the other hand, of the 552 events labelled p A_1^- or p A_2^- by the prism plot analysis and belonging to the 3π mass region considered here, 43% have the decay properties

expected for 2^+, and 14% those for a 1^+ signal. Thus there are more than 40% of the events which must be classified as background coming from other channels.

4. PROPERTIES OF THE $\Delta^{\circ}\rho^{\circ}$ CHANNEL

The $\langle Y_L^M \rangle$ for the Δ° and ρ° resonances are used to compute the density matrix elements which characterize the production of this process as a function of t'. The results are given in table 5.

All illegal moments were found compatible with zero. To estimate the efficiency of the prism-plot separation, we have computed the same density matrix elements for the sample of events obtained by mass cuts on the $\pi^+\pi^-$ and $p\pi^-$ spectra :

$$0.680 < M(\pi^+\pi^-) < 0.860 \text{ GeV}$$
$$1.160 < M(p\pi^-) < 1.280 \text{ GeV}$$

This comparison is made in figure 5, where we also show the results obtained by Barnham et al., [6] on the reaction : $\pi^+ p \to \Delta^{++}\rho^{\circ}$ at 3.7 GeV/c. We see that the three sets of values are in general in good agreement.

Both $\pi^+ p \to \Delta^{++}\rho^{\circ}$ and $\pi^- p \to \Delta^{\circ}\rho^{\circ}$ productions can be expressed in terms of I=1 and I=2 t-channel exchanges, the interference term having opposite signs the comparison is valid if the I=2 amplitude and the interference is small, as it is expected.

We have also computed the so-called "class A" relationships for the transversity amplitudes [7], using again the $\Delta^{\circ}\rho^{\circ}$ sample defined by the prism-plot and by mass-cuts, with the additional condition that $t' < 0.10 \text{ GeV}^2$. These relations are given in table 6 and the results presented on figure 6. Again the two samples give comparable results, the prism-plot sample showing however a larger deviation from zero for A2 and A4.

5. CONCLUSIONS

We have shown that at 4 GeV/c, the separation of the four-body final state $p\pi^+\pi^-\pi^-$ into its constituant intermediate channels is still crude even using the seven variable prism plot analysis. The degree of separation fluctuates between 10% and 30% for the different channels. For the $p A_2^-$ channel the spin parity analysis indicates serious losses and contaminations so that it is difficult to estimate the biases which the method introduces in the physics properties of the channel. An analysis of the polarisation of the $\Delta^{\circ}\rho^{\circ}$ channel yields similar results as those obtained by a simple mass cut.

At this energy and for such a complex final state, it is clear that any improvement in the channel separation must be based on a better understanding of the clustering in the multidimensional space, in particular for the regions, where several channels overlap and the interference effects might play an important role.

REFERENCES

[1] F.T. Dao, M.F. Hodous, I.A. Pless and R.A. Singer, Data Analysis PEPR Programing Note. Physics No. 101, January 1971.

J.E. Brau, F.T. Dao, M.F. Hodous, I.A. Pless and R.A. Singer, Phys. Rev. Letter, 27 (1971) 1181.

B. Haves, H.F. Hodous, I.A. Pless and R.A. Singer, "Prism Plot Analysis of the reaction $\pi^+ p \to p\pi^+\pi^-\pi^+$ at 3.9 GeV/c". Submitted to Phys. Rev. Letter.

V. Kistiakowsky, B. Haver, I.A. Pless, J. Wolfson and R.A. Singer, "ρ^o, f^o and Δ^- production in $\pi^- p$ interactions at 3.9 GeV/c". Philadelphia Meson Conference, April 1972.

[2] V. Chaloupka, L. Dobrzynski, A. Ferrando, M.J. Losty, L. Montanet, E. Paul, D. Yaffe and A. Zieminski. Phys. Letters 44B, (1973) 211.

[3] M.J. Losty et al., "A study of $\pi^-\pi^-$ scattering from $\pi^- p$ interactions at 3.93 GeV/c". CERN/D.Ph.II/73. To be submitted to Nucl. Phys.

[4] A. Ferrando et al., "A multidimensional analysis of 3 and 4 body processes at 4 GeV/c". CERN, TC, unpublished.

[5] M. Abramovich, H. Blumenfeld, F. Bruyant, U. Chaloupka, S.U. Chung, J. Diaz, L. Montanet, S. Reucroft and J.A. Rubio, Nucl. Phys. 23B, (1970) 466.

[6] K.W.J. Barnham, G.S. Abram, W.R. Butter, G. Goldhaber, B.H. Hall and J. Mac. Naughton LBL-960, JUNE 1972.

K.W.J. Barnham "Joint decay correlations in $\pi^+ p \to V^o \Delta^{++}$ reactions at 3.7 GeV/c". Invited paper presented at the "III^e Rencontre de Moriond sur les interactions électromagnétiques", March 1972.

[7] A. Bialas and K. Zalewski, Nucl. Phys. 6B, (1968) 465.

TABLE CAPTIONS

1. Mass and width used for the resonances and mass spectrum used for the $(p\pi^+\pi^-)$ diffraction dissociation.

2. Definition of the variables and of their range (in MeV/c) for our events.

   $\vec{p}$: momentum (CMS)

   q : longitudinal momentum (CMS)

   T : Kinetic energy (CMS)

3. Number of events attributed to each channel after 13 iterations of the prism-plot analysis.

4. Spin-parity analysis of the 3π system in region

   $1.30 < M(3\pi) < 1.34$ GeV.

5. Density matrix elements for Δ^o and ρ^o of the channel $\Delta^o\rho^o$ separated by the prism-plot analysis.

6. Relations of Biales and Zalewski for the transversity amplitudes of the $\Delta^o\rho^o$ channel.

RESONANCE	M	Γ
ρ	765	135
Δ^{o}	1236	120
N^{*}_{1520}	1520	120
N^{*}_{1688}	1688	120
A_1	1100	200
A_2	1310	100
f^{o}	1250	140
DD[8]	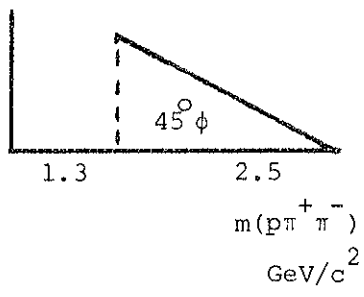	

TABLE 1

Mass and width used for resonances and mass shape for DD.

VARIABLE	MIN. VALUE	MAX. VALUE	RANGE
$t^{P}_{\pi^-\pi^-} = \sqrt{(P_{\pi^-_1} + P_{\pi^-_2})^2}_{t}$	0	1169	1169
$X_{VH} = \frac{1}{4}(3q_p - (q_{\pi^+} + q_{\pi^-} + q_{\pi^-_2}))$	-1195	1154	2349
$Y_{VH} = \frac{1}{2\sqrt{2}}(2\,q_{\pi^+} - (q_{\pi^-_1} + q_{\pi^-_2}))$	-982	999	1981
$Z_{VH} = \sqrt{\frac{2}{3}}\,(q_{\pi^-_1} - q_{\pi^-_2})$	-1019	1029	2048
$X_{ES} = \frac{1}{4}\,(3T_p - (T_{\pi^+} + T_{\pi^-_1} + T_{\pi^-_2}))$	-378	232	610
$Y_{ES} = \frac{1}{2\sqrt{2}}\,(2T_{\pi^+} - (T_{\pi^-_1} + T_{\pi^-_2}))$	-523	701	1224
$Z_{ES} = \sqrt{\frac{2}{3}}\,(T_{\pi^-_1} - T_{\pi^-_2})$	-612	610	1222

TABLE 2

Explicit form and variation field of the seven Prism Plot variables used in the $\pi^- p \to p\pi^+\pi^-\pi^-$ sample. (Quantities in MeV/c).

	RATES (%)	Number of events	CONTAMINATIONS COMING FROM OTHER CHANNELS (IN NB. OF EVENTS)										Lower Limit for Total losses
			$p^{A}1$	$p^{A}2$	$N^{*}_{1520}\rho^{o}$	$N^{*}_{1688}\rho^{o}$	$\Delta^{o}\rho^{o}$	$\Delta^{++}\pi^{-}\pi^{-}$	$DD(\Delta^{+}\pi\pm)\pi^{-}$	$DD(p\pi^{+}\pi^{-})\pi^{-}$	$p\pi^{-}f^{o}$	ph. sp.	
$p^{A}1$	13.1	2538			0	15	20	0	0	0	0	0	35
$p^{A}2$	11.7	2267			15	0	20	40	68	0	0	18	161
$N^{*}_{1520}\rho$	8.5	1654	75	46		20	0	20	0	0	0	0	161
$N^{*}_{1688}\rho$	10.7	2077	100	25	0		0	40	0	0	0	0	165
$\Delta^{o}\rho$	11.9	2313	50	70	0	66		50	?	0	0	0	236
$\Delta^{++}\pi^{-}\pi^{-}$	9.2	1793	250	46	104	130	130		?	?	42	30	902
$DD(\Delta^{++}\pi^{-})\pi^{-}$	17.5	3409					?						?
$DD(p\pi^{+}\pi^{-})\pi^{-}$	10.5	2050											?
$p\pi^{-}f^{o}$	3.7	728	?	?	20	20	46	0	0	0		0	86
ph.sp.	3.1	614											1746 / 1746
Lower limit for total contamination			475	187	139	251	386	150	68	0	42	48	

TABLE 3

RATES AND CONTAMINATIONS AFTER 13 ITERATIONS

? Not able to estimate

O No apparent contamination

CHANNEL	Σ weights	2^+	$1^+/s$	$1^+/d$	$0^-/oo$	%ρπ	% background
ALL CHANNELS ≡ ALL DATA	1139	321 ± 43	233 ± 42	13 ± 13	386 ± 47	49 ± 3	51 ± 3
$pA_1 + pA_2$	552	235 ± 22	64 ± 21	28 ± 17	43 ± 46	57 ± 4	43 ± 4
$N^*_{1520}\rho$	59	16 ± 6	10 ± 6	3 ± 5	33 ± 5	47 ± 9	53 ± 9
$N^*_{1688}\rho$	77	21 ± 8	21 ± 8	-	36 ± 6	55 ± 8	45 ± 8
$\Delta^0_{1236}\rho$	112	7 ± 12	51 ± 14	9 ± 9	45 ± 10	58 ± 6	42 ± 6
$\Delta^{++}\pi^-\pi^-$	78	9 ± 4	5 ± 5	6 ± 6	27 ± 7	25 ± 8	75 ± 8
$DD(\Delta^{++}\pi^-)\pi^-$	139	26 ± 9	13 ± 9	11 ± 8	45 ± 10	27 ± 5	73 ± 5
$DD(p\pi^+\pi^-)\pi^-$	88	-	-	6 ± 3	60 ± 10	8 ± 6	92 ± 6
$p\pi - f^0$	4	-	-	-	-	-	-
ph.sp	30	-	-	-	-	-	-
Only ρ producing channels.	844	295 ± 33	198 ± 33	25 ± 22	235 ± 35	60 ± 4	40 ± 4

TABLE 4

J^P analysis of 3π-system. Region 1.30 GeV/c^2 $\leq M_{3\pi} \leq$ 1.34 GeV/c^2

t' GeV^2	0.0-0.01	0.01-0.025	0.025-0.045	0.045-0.07	0.07-0.11	0.11-0.18	0.18-0.34	0.34-1.0
Number of events	128	161	195	209	257	353	390	414
ρ^{00}	.753±.068	.712±.060	.802±.057	.757±.054	.730±.049	.728±.042	.688±.040	.507±.038
Re ρ^{10}	.009±.044	-.024±.039	-.002±.035	-.075±.035	-.067±.030	-.097±.026	-.066±.023	-.045±.022
ρ^{1-1}	-.073±.047	.023±.041	-.003±.036	-.042±.034	.024±.034	-.040±.029	.049±.028	.092±.030
ρ_{33}	.144±.053	.170±.046	.174±.041	.115±.043	.174±.037	.160±.031	.119±.030	.205±.028
Re ρ_{31}	.062±.045	.081±.043	.020±.039	.043±.037	.018±.035	.093±.030	.056±.028	.017±.026
ρ_{3-1}	.030±.045	-.004±.043	.048±.038	.086±.037	.001±.034	.074±.025	.074±.025	.117±.026

TABLE 5

Density matrix elements for Δ^0 and ρ^0 in the $\Delta^0\rho^0$ Prism Plot selected channel.

A.1	$T^{20}_{00} = \sqrt{2}\, T^{02}_{00}$
A.2	$\mathrm{Re}\ T^{22}_{20} = \frac{1}{2}\ \mathrm{Re}\ T^{20}_{20}$
A.3	$\mathrm{Re}\ T^{22}_{02} = \frac{1}{2}\ \mathrm{Re}\ T^{02}_{02}$
A.4	$T^{22}_{00} = \frac{1}{2\sqrt{6}} - \frac{1}{\sqrt{2}}\ T^{02}_{00}$
A.5	$\mathrm{Im}\ T^{22}_{20} = \frac{1}{2}\ \mathrm{Im}\ T^{20}_{20}$
A.6	$\mathrm{Im}\ T^{22}_{02} = \frac{1}{\sqrt{2}}\ \mathrm{Im}\ T^{02}_{02}$

TABLE 6

Biatas and Zalewski quark model class A relationship in transversity frames.

FIGURE CAPTIONS

Fig. 1 Mass spectra for the total sample: $\pi^- p \to p\pi^+\pi^-\pi^-$.

a) $\pi^+\pi^-$ effective mass

b) $p\pi^+$ effective mass

c) $p\pi^-$ effective mass

d) $\pi^+\pi^-\pi^-$ effective mass

e) $p\pi^+\pi^-$ effective mass

Fig. 2 Mass spectra for some of the channels separated by the prism-plot analysis after 13 iterations:

a) $\pi^+\pi^-\pi^-$ effective mass for the p A_1 channel.

b) $\pi^+\pi^-\pi^-$ effective mass for the p A_2 channel.

c) $\pi^+_a\pi^-_b\pi^-_c$ effective mass for the p A_2 channel, $A_2 \to \rho\pi^-_c$, $\rho \to \pi^+_a\pi^-_b$

d) $p\pi^-_b$ effective mass for the $\Delta^0\rho^0$ channel. $\Delta^0 \to p\pi^-_b$ $\rho^0 \to \pi^+_a\pi^-_c$

e) $\pi^+_a\pi^-_c$ effective mass for the $\Delta^0\rho^0$ channel, $\Delta^0 \to p\pi^-_b$, $\rho^0 \to \pi^+_a\pi^-_c$

f) $p\pi^+_a$ effective mass for the $\Delta^{++}\pi^-\pi^-$ channel.

g) $\pi^-\pi^-$ effective mass for the $\Delta^{++}\pi^-\pi^-$ channel.

h) $p\pi^+_a\pi^-_b$ effective mass for the DD($p\pi^+_a\pi^-_b$) π^-_c channel.

Fig. 3 Production angle for several channels separated by the prism-plot analysis after 13 iterations.

a) $\cos\theta^*(p,p)$ for the p A_1 channel.

b) $\cos\theta^*(p,p)$ for the p A_2 channel.

c) $\cos \theta^*(p, \Delta^o)$ for the $\Delta^o\rho^o$ channel.

d) $\cos \theta^*(p, \Delta^{++})$ for the $\Delta^{++}\pi^-\pi^-$ channel.

e) $\cos \theta^*(p, N^*(1520))$ for the $N^*(1520)\rho^o$ channel.

f) $\cos \theta^*(p, N^*(1680))$ for the $N^*(1680)\rho^o$ channel.

Fig. 4 Effective masses after separation by the prism-plot analysis:

a) $p\pi^+$ effective mass for the $p\ A_1$ channel.

b) $p\pi^-$ effective mass for the $p\ A_1$ channel.

c) $p\pi^+$ effective mass for the $p\ A_2$ channel.

d) $p\pi^+$ effective mass for the $\Delta^o\rho^o$ channel.

Fig. 5 Density matrix elements ρ_{oo}, Re ρ_{1o}, ρ_{1-1} for ρ^o, ρ_{33}, $\mathrm{Re}\rho_{31}$, ρ_{3-1} for Δ, computed in the t-channel helicity frame (Gottfried-Jackson-frame), for the channel $\pi^{\pm}p \to \Delta\rho^o$. Three sets of values are given. The dots represent the values obtained for $\Delta^o\rho^o$ separated by the prism-plot analysis. The triangles represent the values obtained for the same reaction separated by mass cuts (see text). The circles reproduce the values obtained by Abrams et al [6] for the reaction $\pi^+p \to \Delta^{++}\rho^o$ at 3.7 GeV/c.

Fig. 6 Check of the Biales-Zalewski relations for the transversity amplitudes which describe the $\Delta^o\rho^o$ channel. The dots represent the values obtained, using the separation given by the prism-plot analysis, the triangles represent the values obtained using mass cut separation (see text).

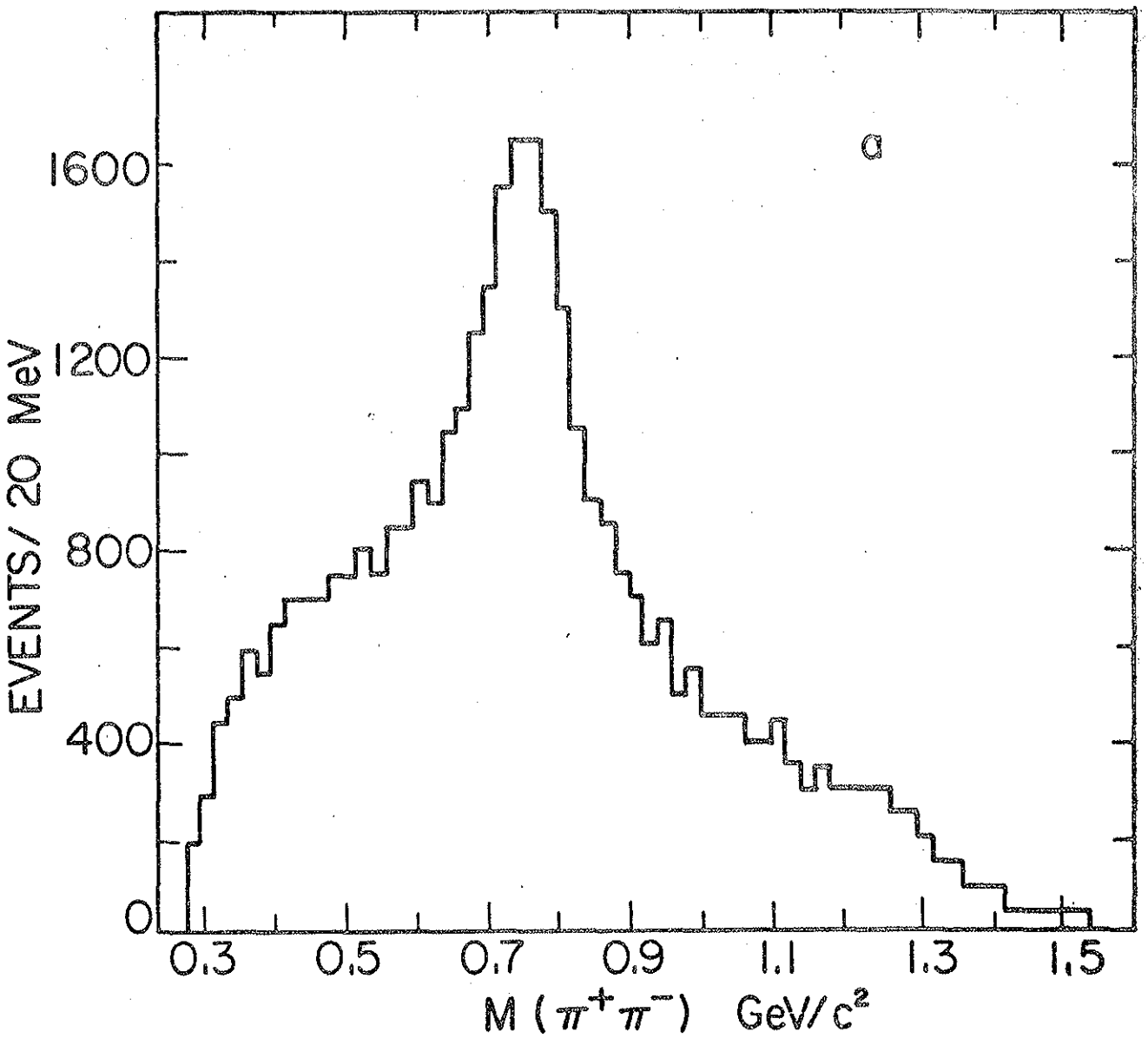
a
1600
1200
800
400
0
EVENTS/ 20 MeV
0.3
0.5
0.7
0.9
1.1
1.3
1.5
M ($\pi^+\pi^-$) GeV/c^2

fig. 1

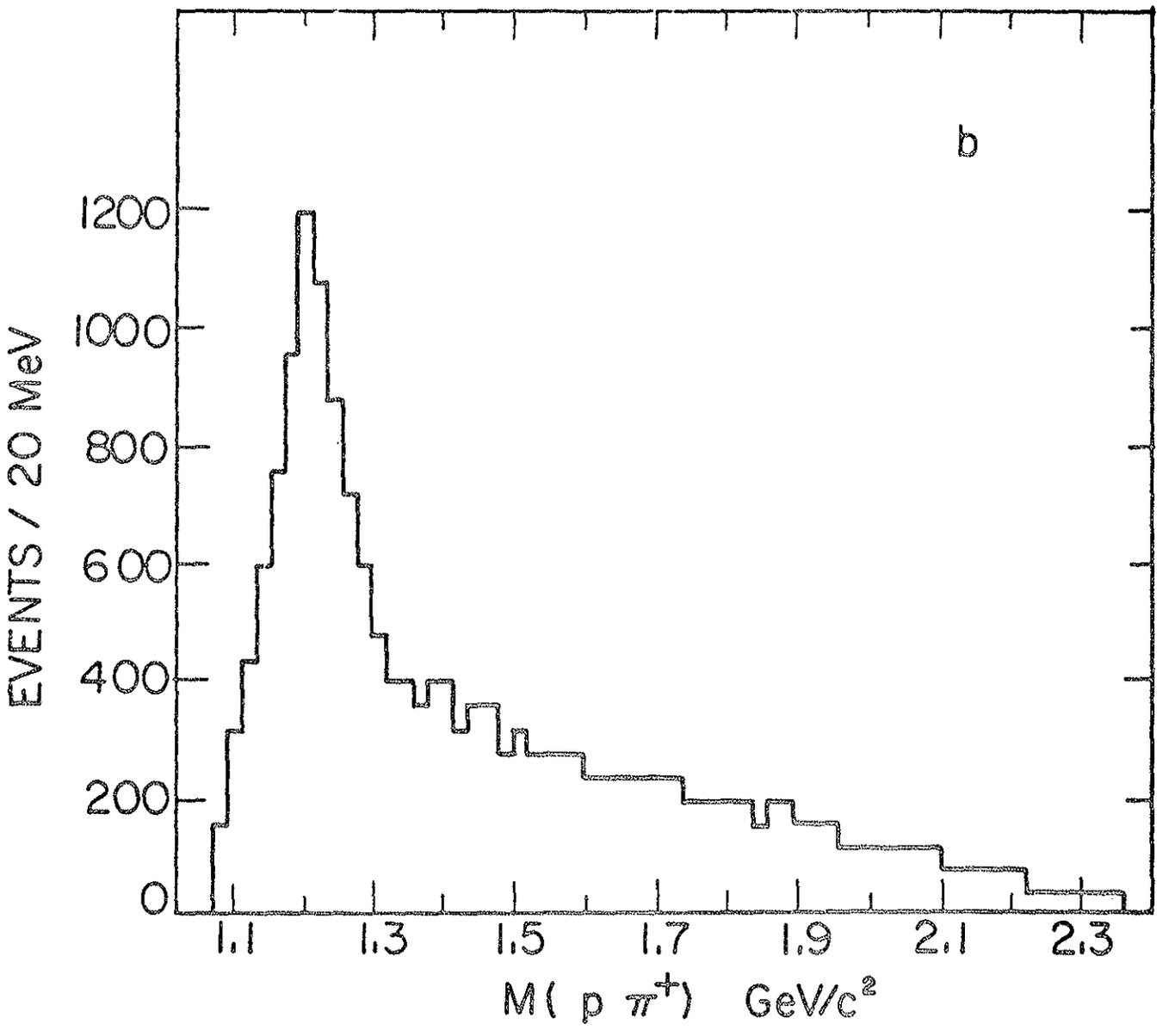
b
EVENTS / 20 MeV
0
200
400
600
800
1000
1200
1.1
1.3
1.5
1.7
1.9
2.1
2.3
M(p π^+) GeV/c^2

fig. 1

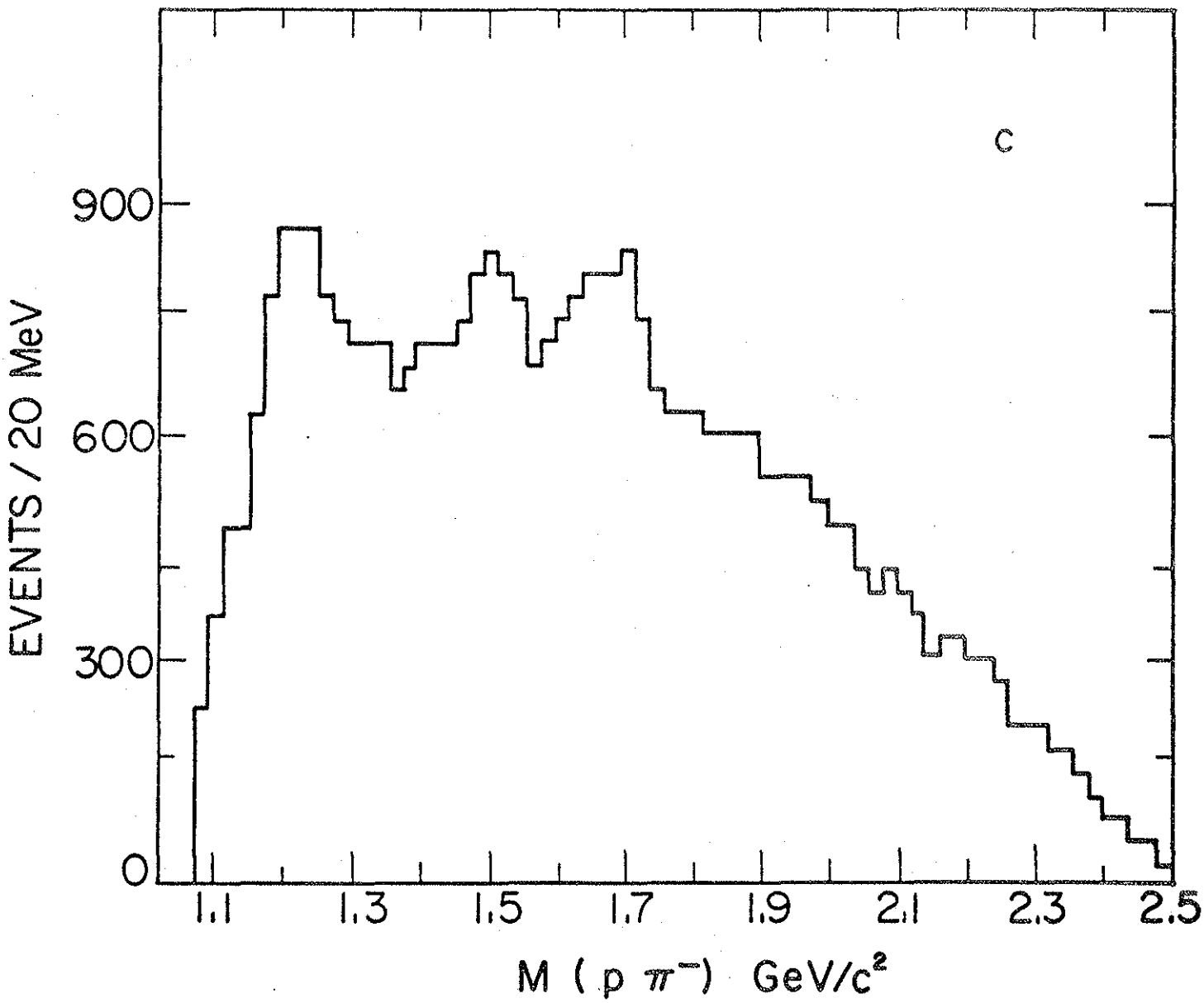

fig. 1

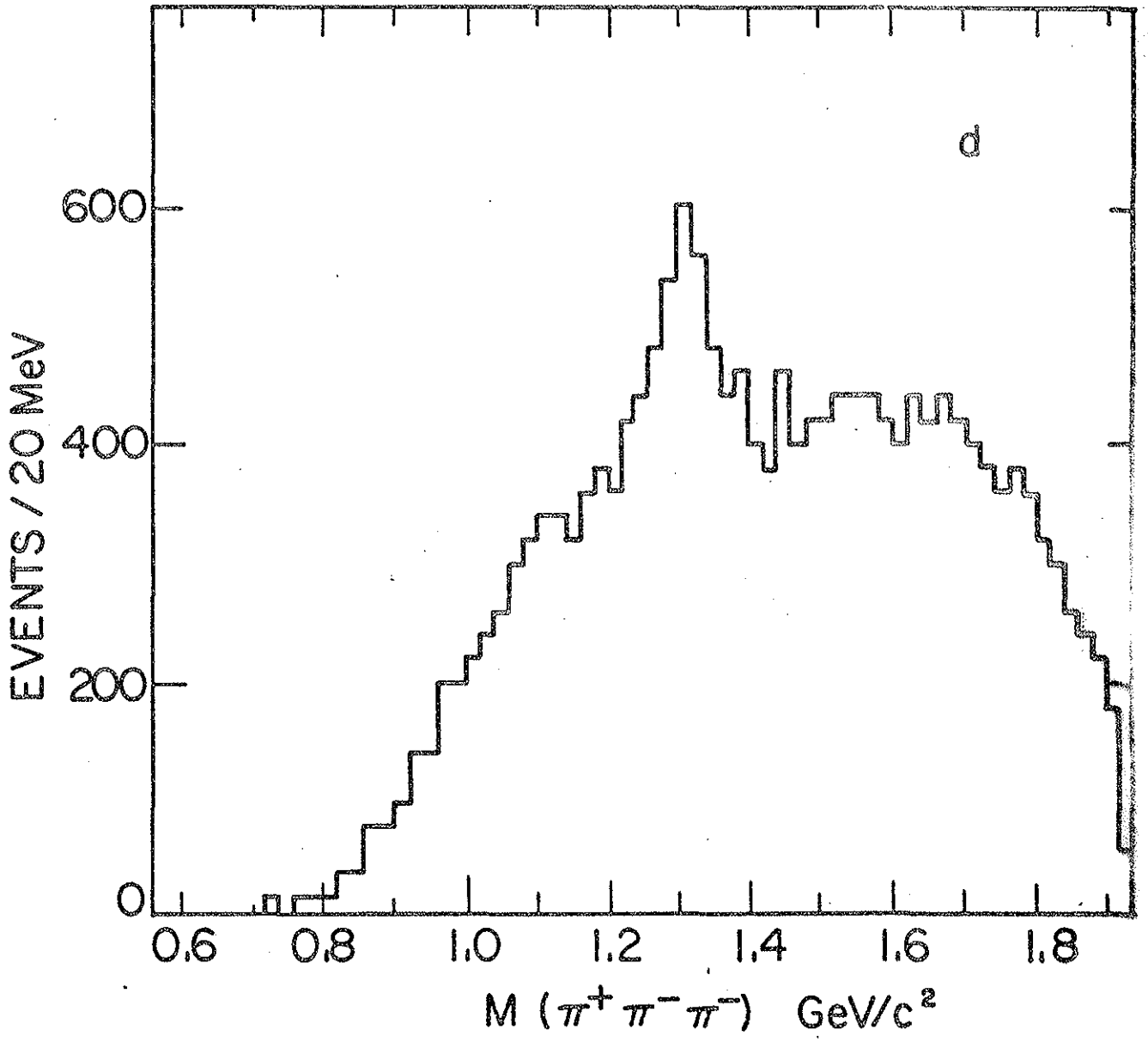

fig. 1

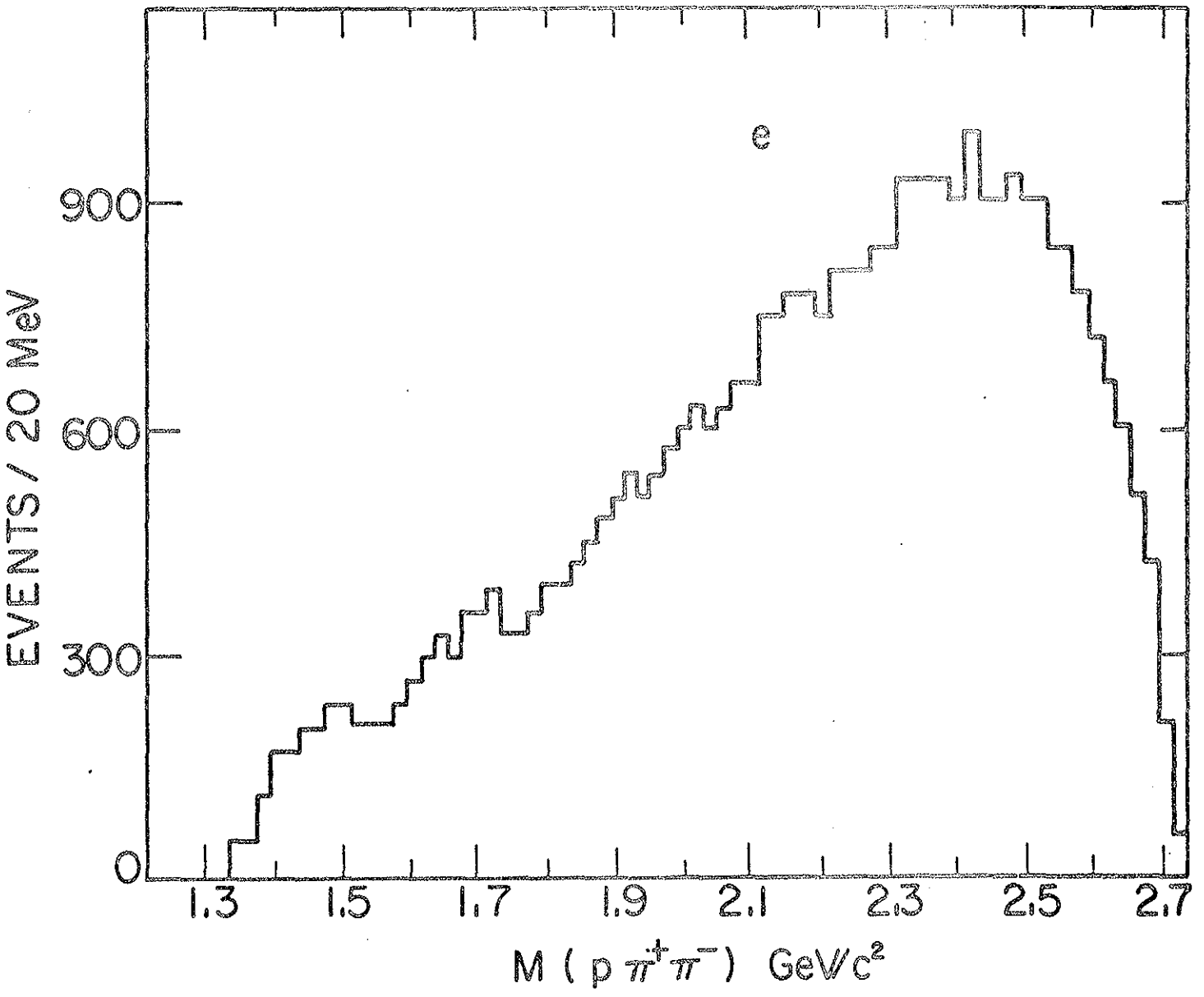

fig. 1

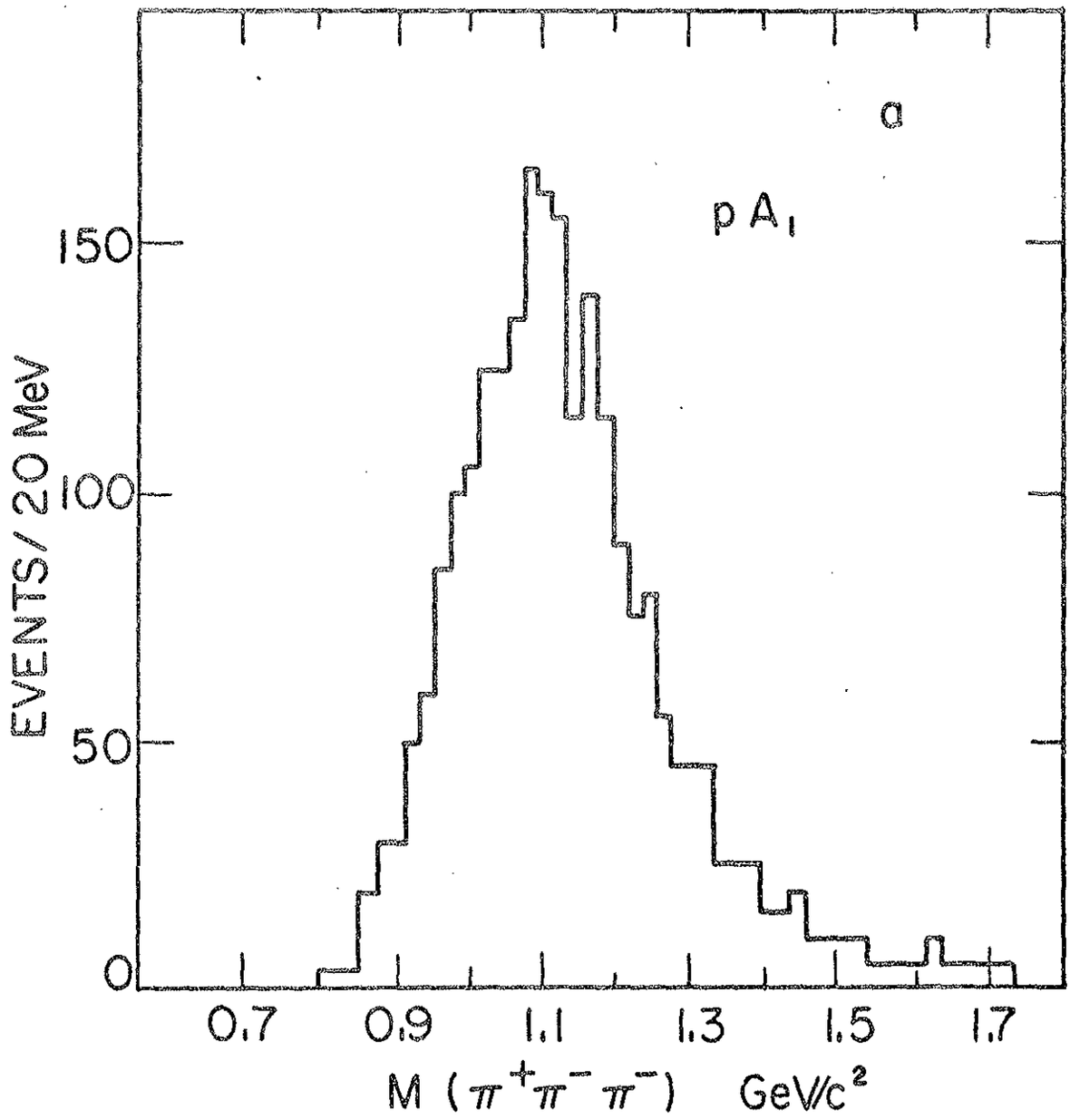

fig. 2

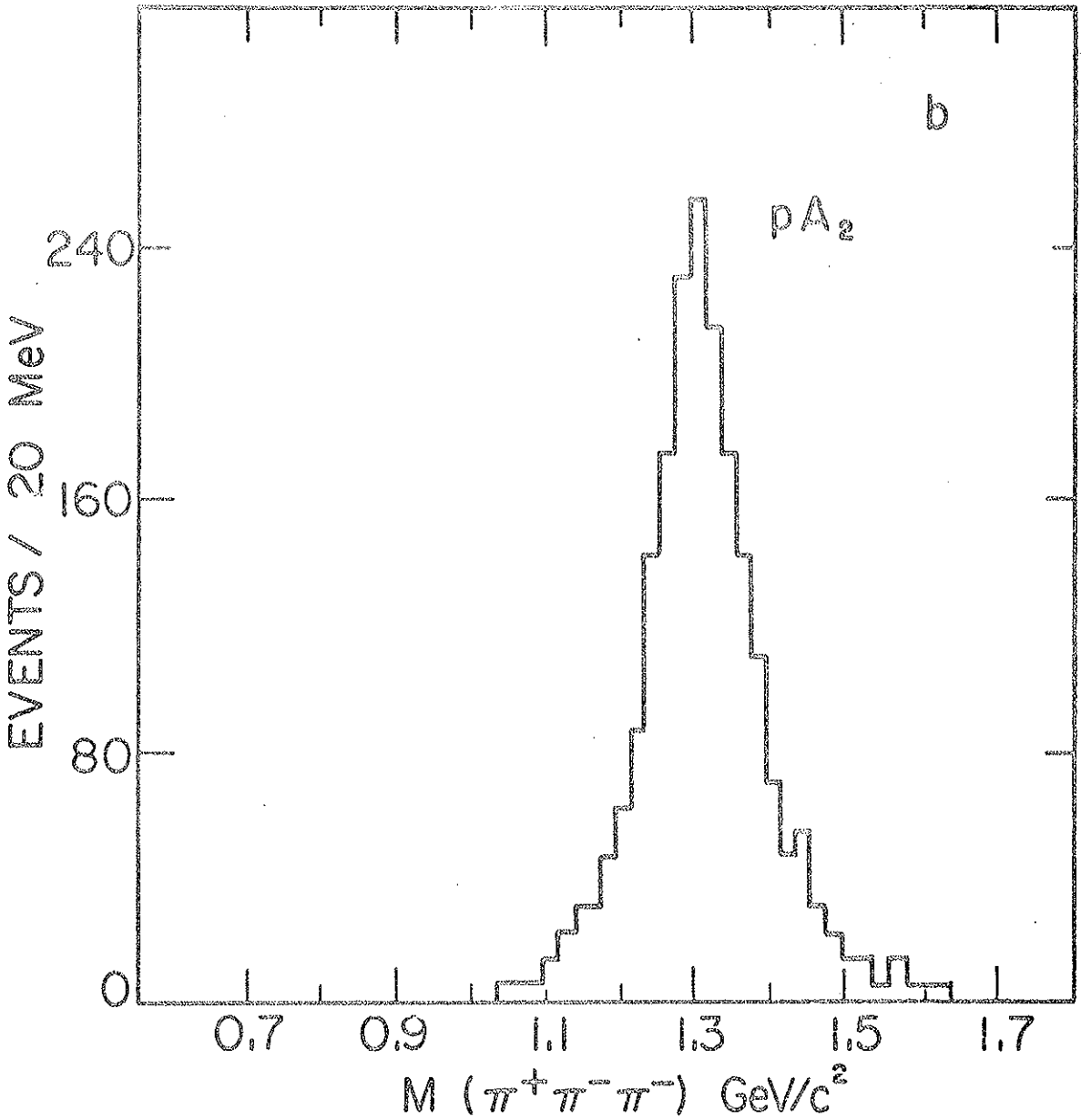

fig.2

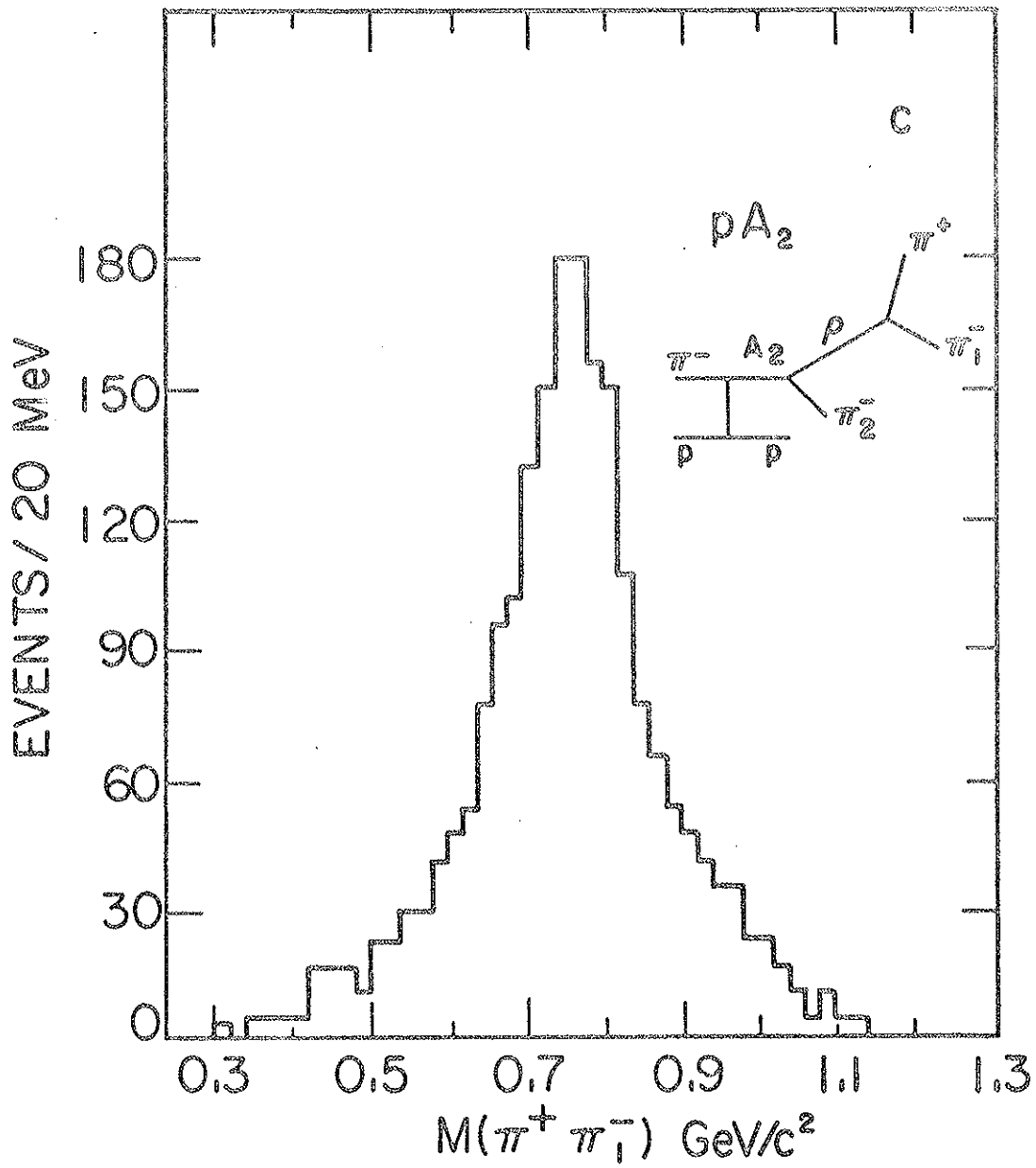
C
pA_2
π^+
ρ
π^-_1
π^-
A_2
π^-_2
p
p
EVENTS / 20 MeV
180
150
120
90
60
30
0
0.3
0.5
0.7
0.9
1.1
1.3
$M(\pi^+\pi^-_1)$ GeV/c^2

fig. 2

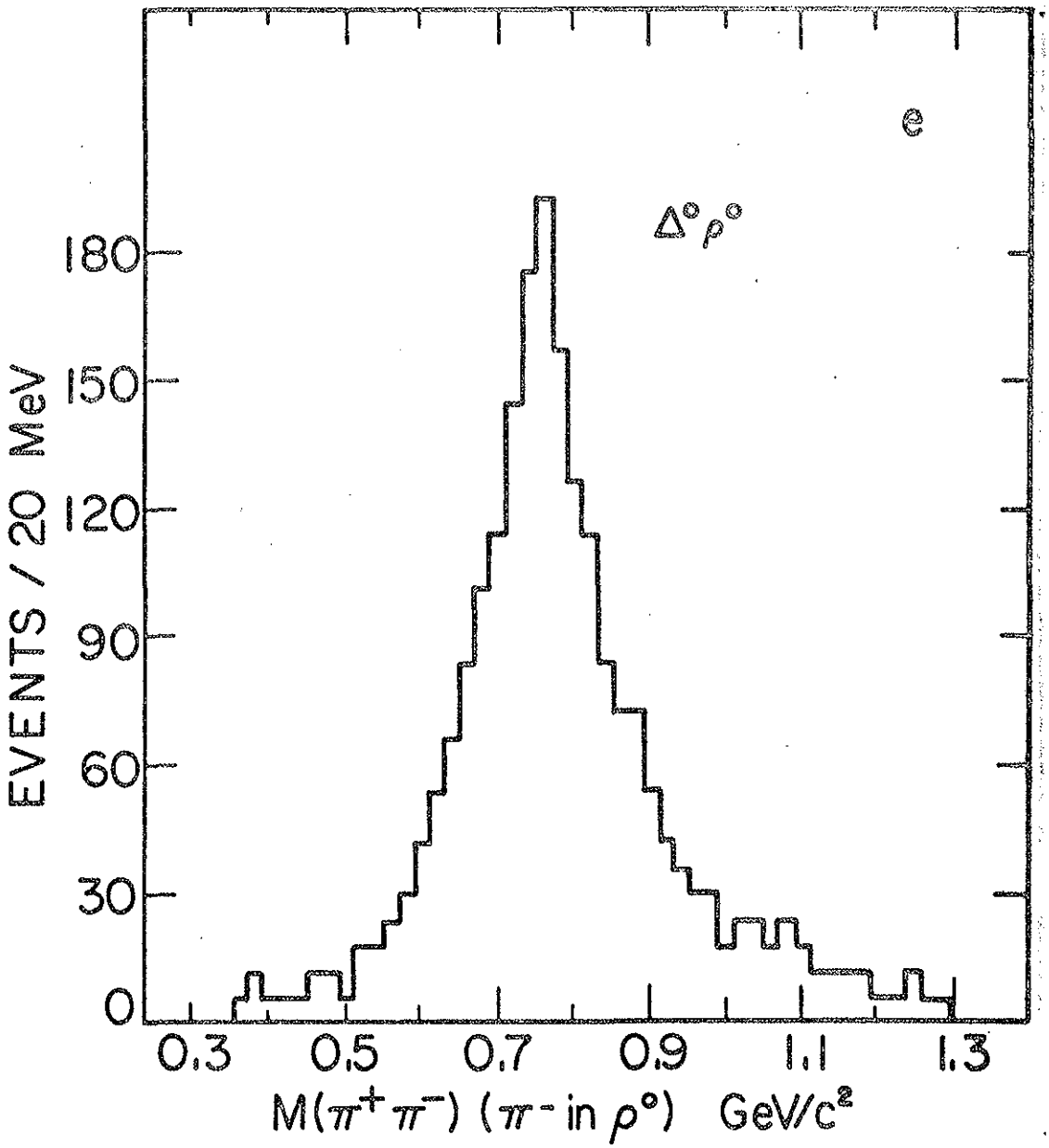
e
Δ°ρ°
EVENTS / 20 MeV
180
150
120
90
60
30
0
0.3
0.5
0.7
0.9
1.1
1.3
M(π⁺π⁻) (π⁻ in ρ°) GeV/c²

fig. 2

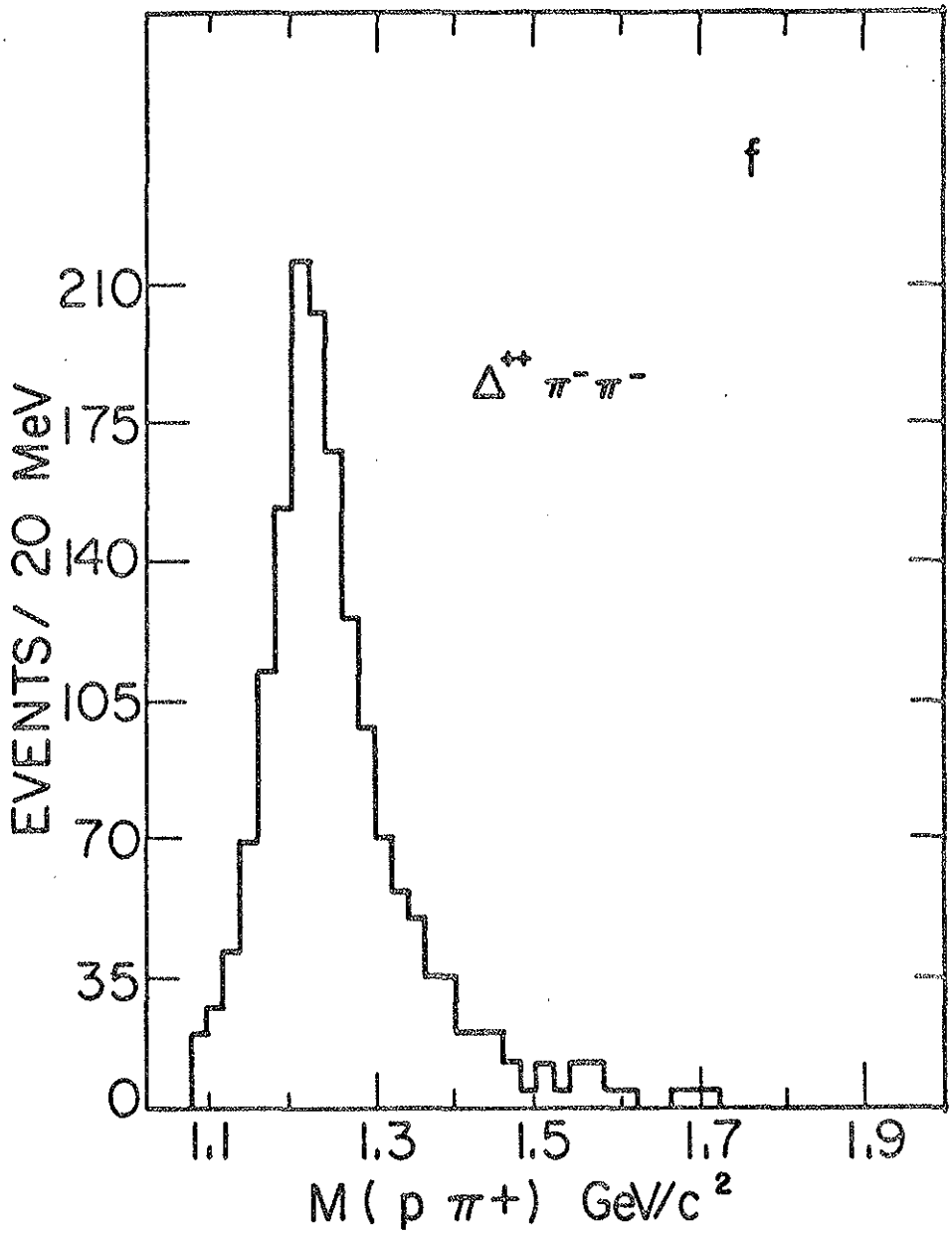
f
$\Delta^{++}\pi^-\pi^-$
EVENTS/ 20 MeV
210
175
140
105
70
35
0
1.1
1.3
1.5
1.7
1.9
M (p π+) GeV/c^2

fig. 2

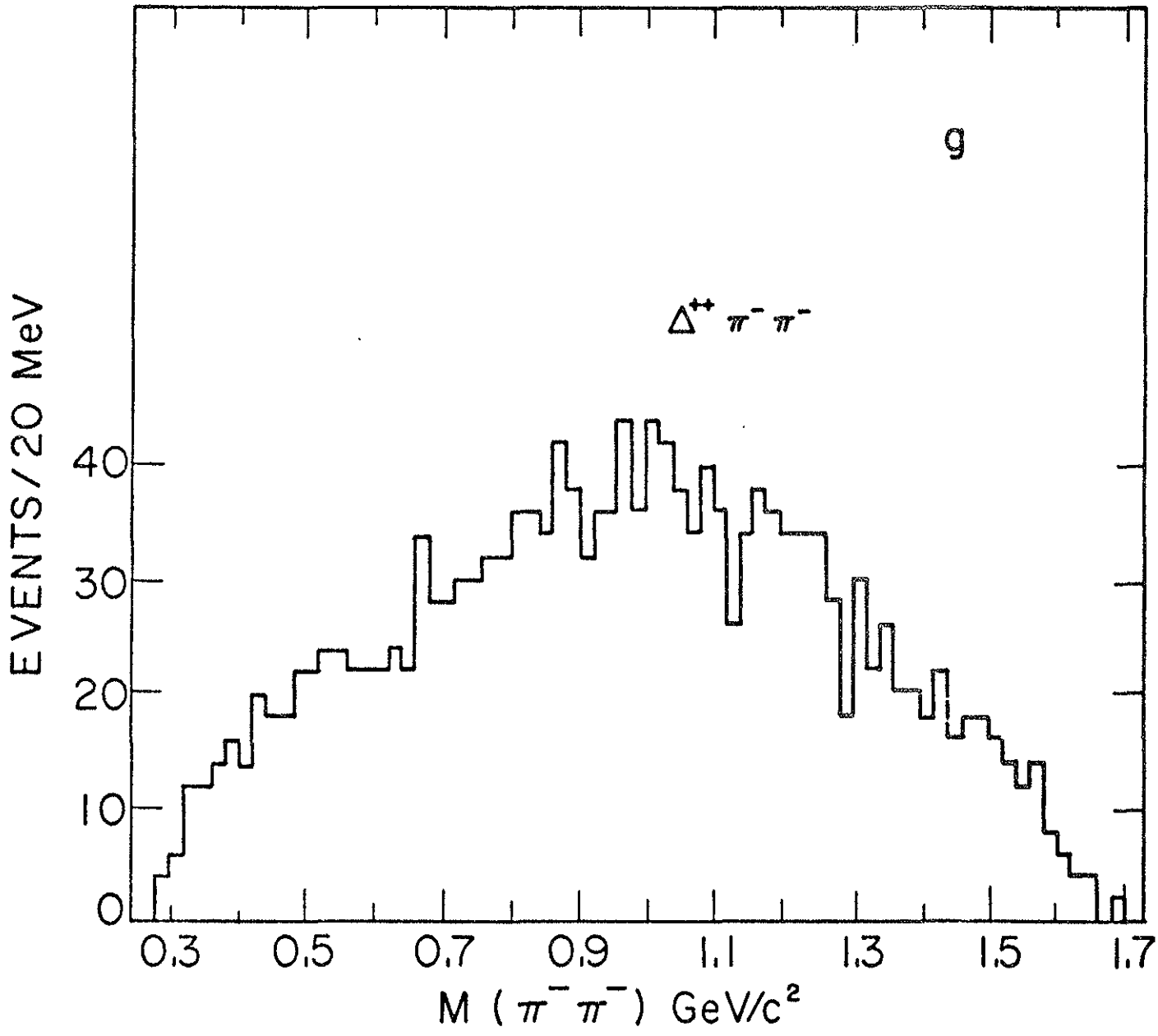
g
$\Delta^{++}\pi^-\pi^-$
EVENTS/20 MeV
0
10
20
30
40
0.3
0.5
0.7
0.9
1.1
1.3
1.5
1.7
M ($\pi^-\pi^-$) GeV/c^2

fig. 2

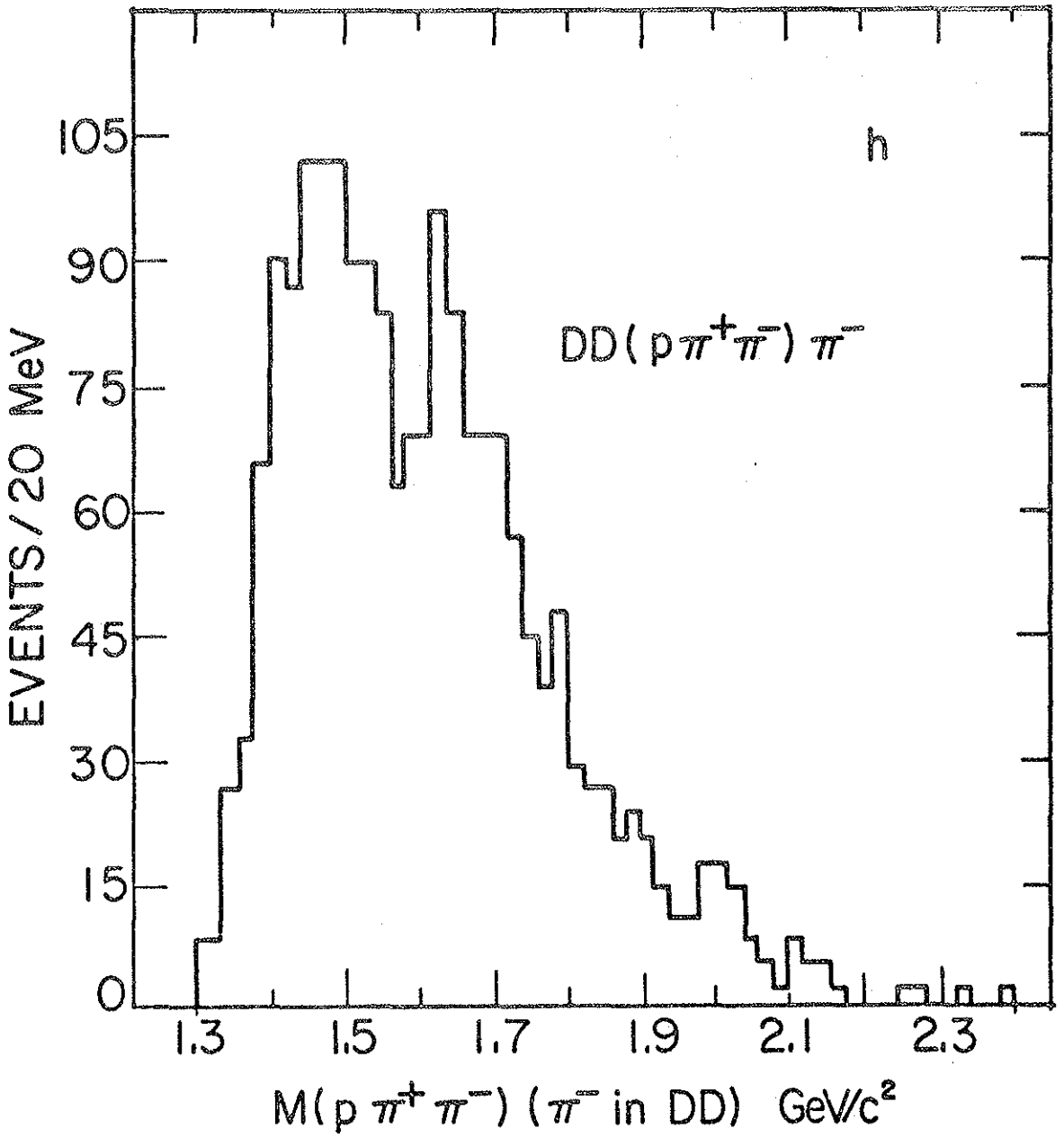
h
DD(p π+ π−) π−
EVENTS / 20 MeV
105
90
75
60
45
30
15
0
1.3
1.5
1.7
1.9
2.1
2.3
M(p π+ π−) (π− in DD) GeV/c²

fig. 2

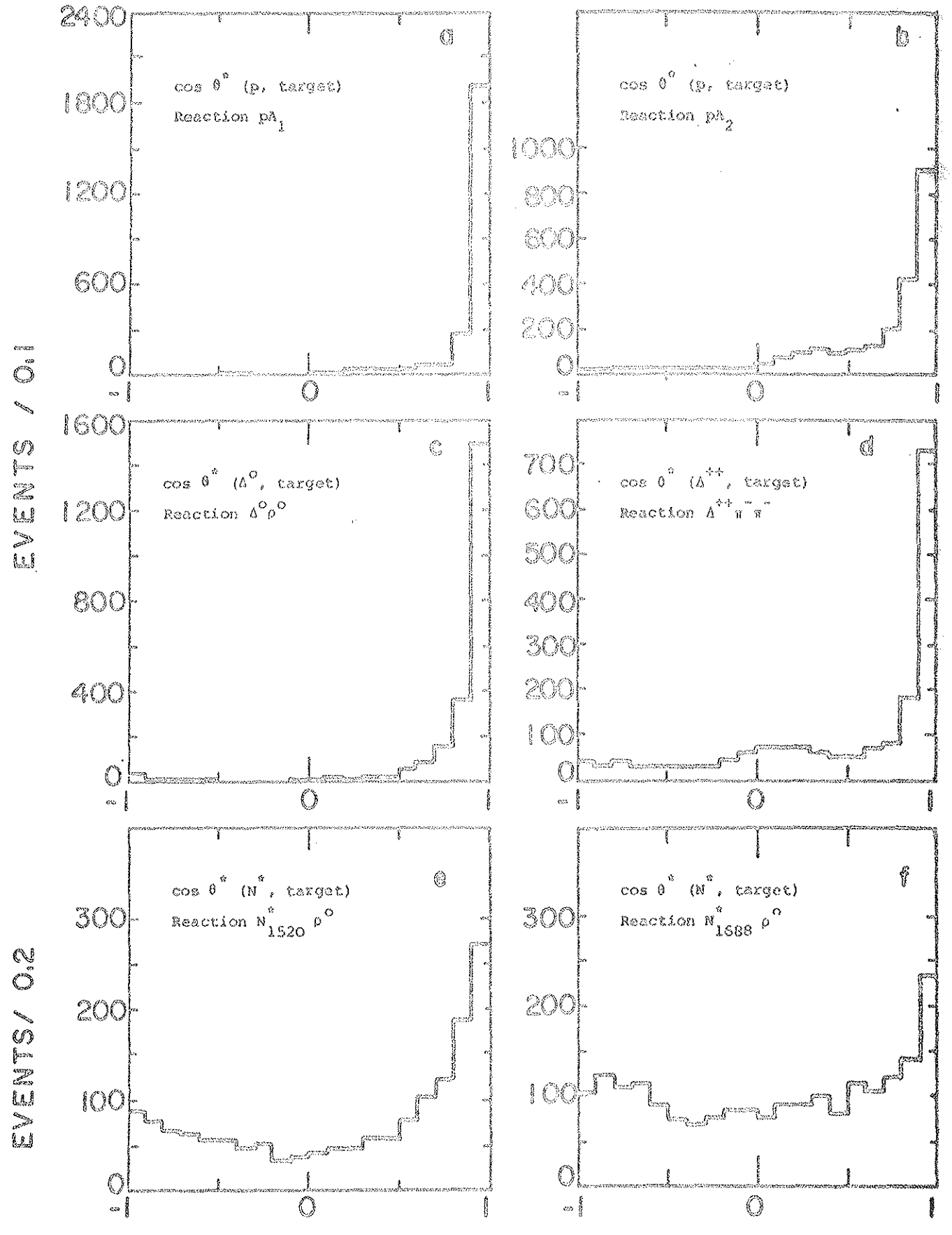
EVENTS / 0.1
EVENTS/ 0.2
a
cos θ* (p, target)
Reaction pΛ1
b
cos θ* (p, target)
Reaction pΛ2
c
cos θ* (Δ°, target)
Reaction Δ°ρ°
d
cos θ* (Δ++, target)
Reaction Δ++π⁻π⁻
e
cos θ* (N*, target)
Reaction N*1520 ρ°
f
cos θ* (N*, target)
Reaction N*1688 ρ°

fig. 3

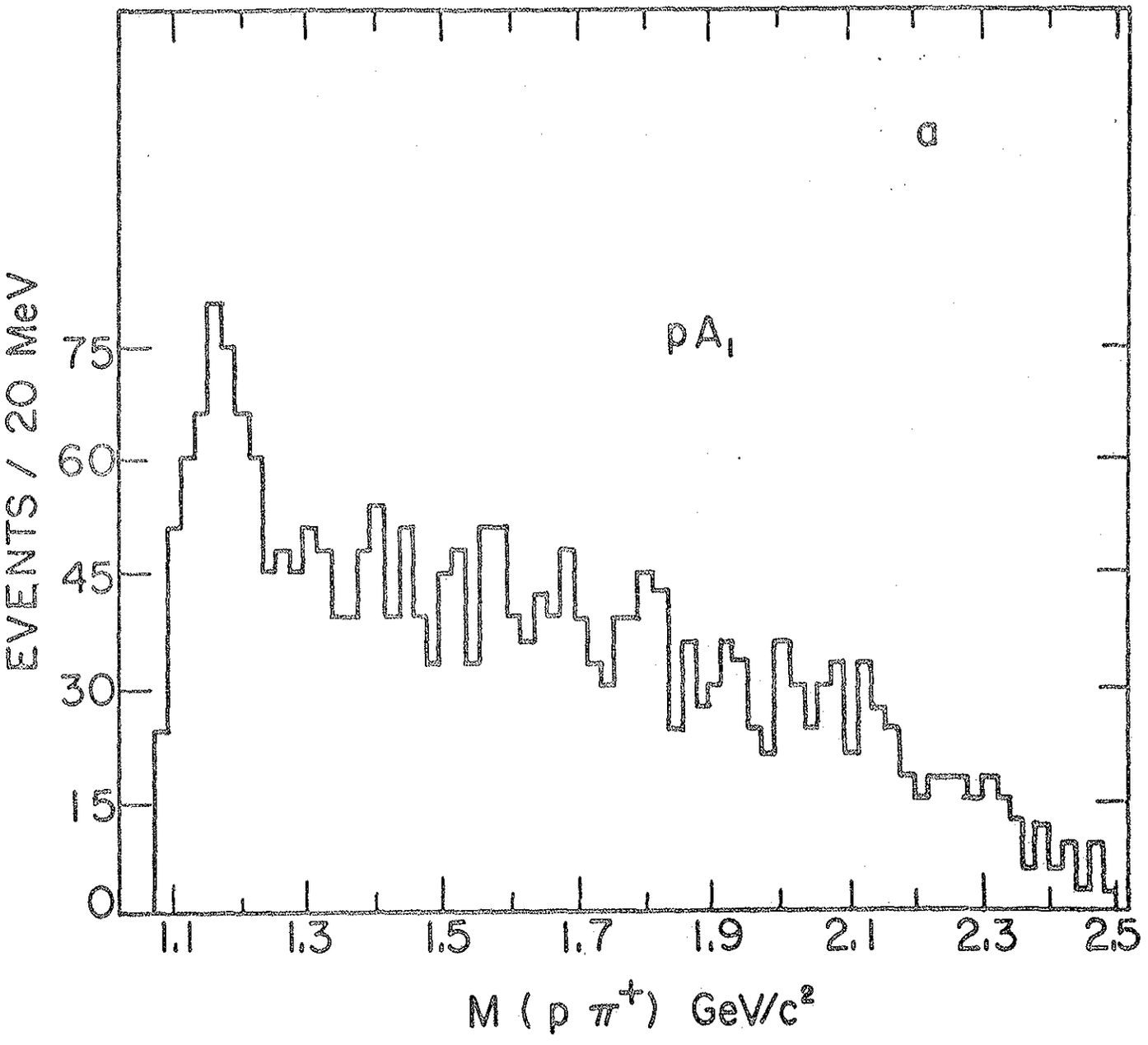
a
pA1
EVENTS / 20 MeV
0
15
30
45
60
75
1.1
1.3
1.5
1.7
1.9
2.1
2.3
2.5
M (p π+) GeV/c²

fig. 4

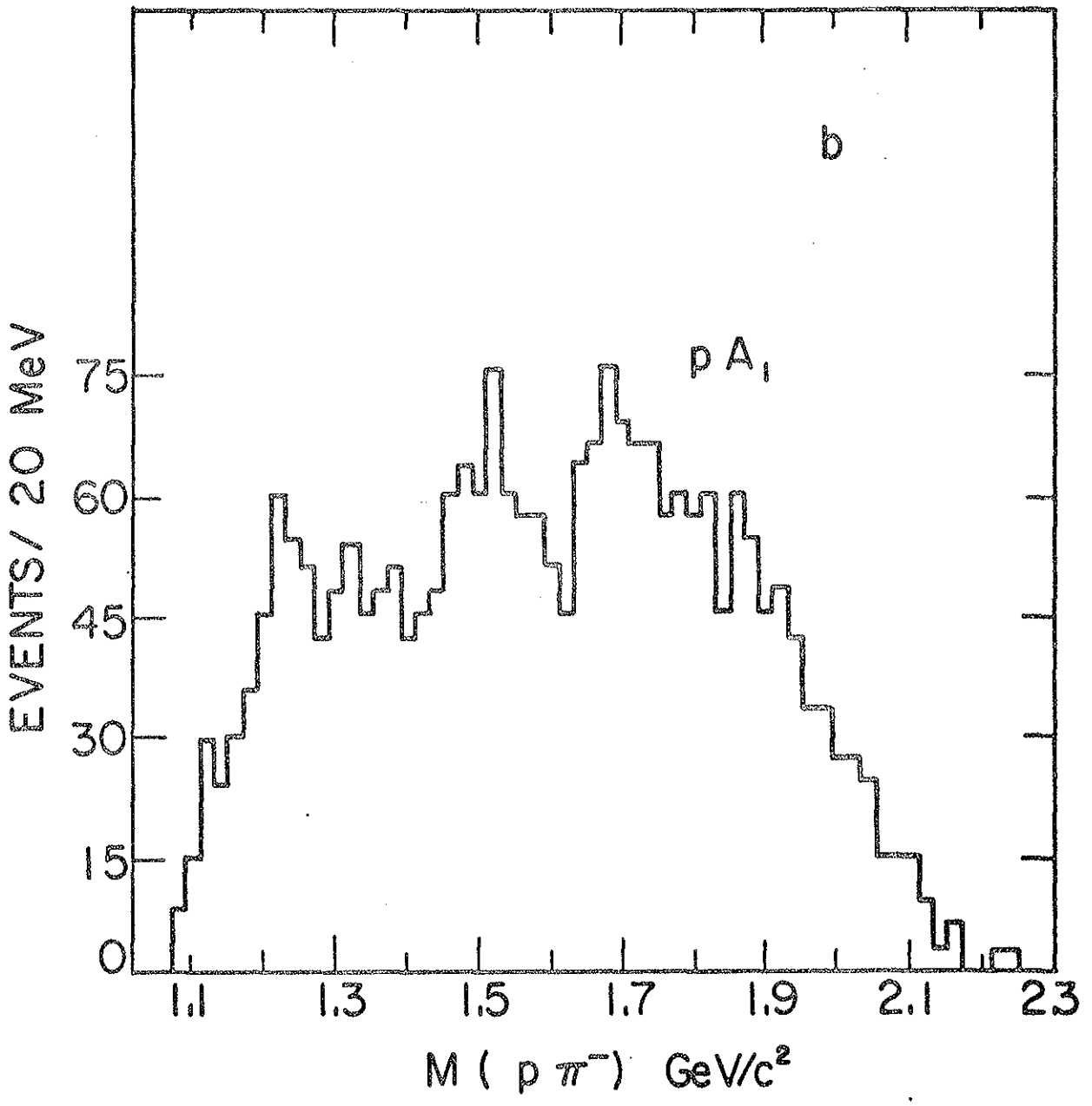

fig. 4

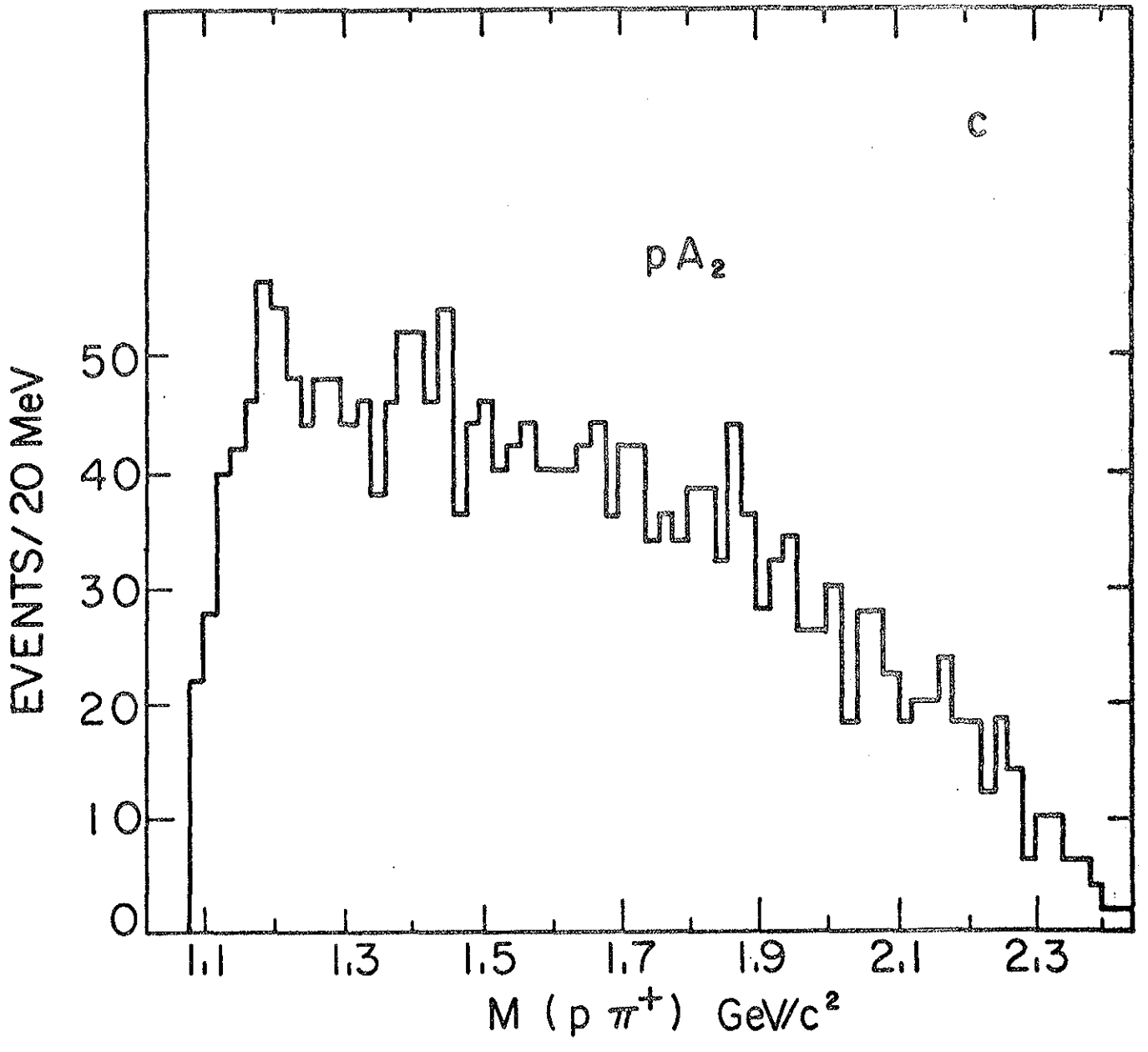

fig. 4

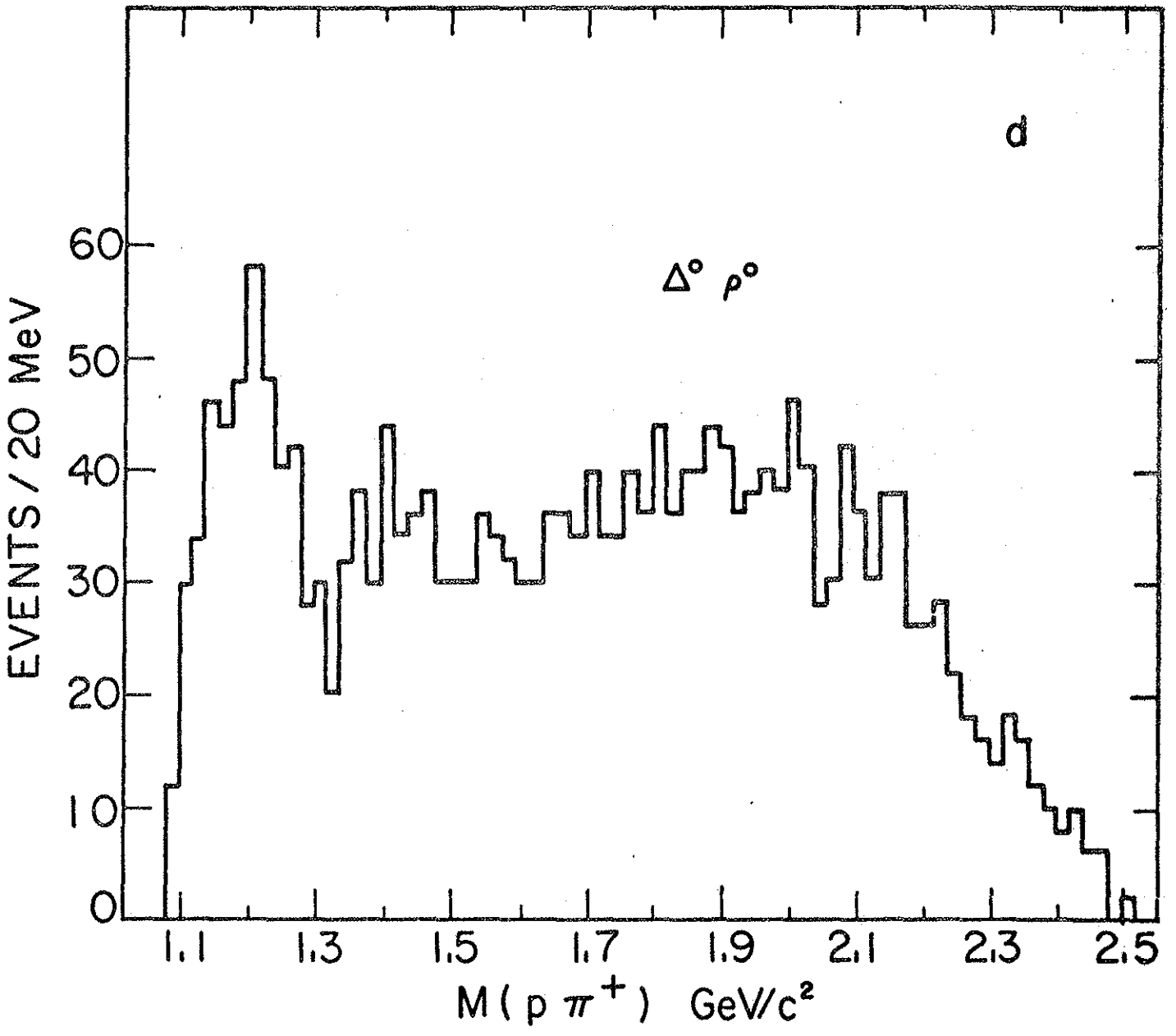
d
Δ° ρ°
EVENTS / 20 MeV
0
10
20
30
40
50
60
1.1
1.3
1.5
1.7
1.9
2.1
2.3
2.5
M (p π+) GeV/c²

fig. 4

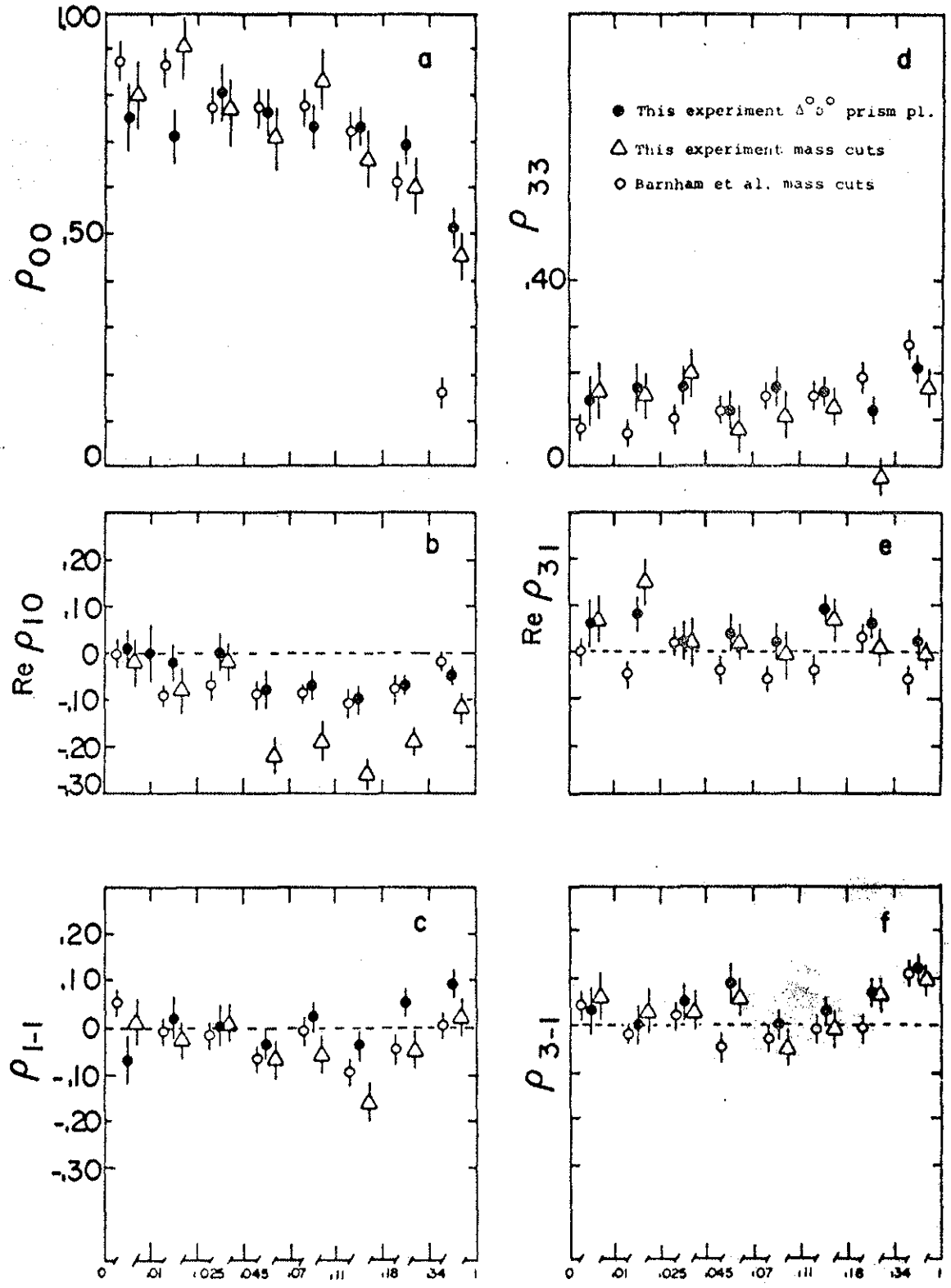
a
b
c
d
e
f
ρ_{00}
Re ρ_{10}
ρ_{1-1}
ρ_{33}
Re ρ_{31}
ρ_{3-1}
1.00
.50
0
.40
.20
.10
-.10
-.20
-.30
.01
.025
.045
.07
.11
.18
.34
1
This experiment $\Delta^{\circ}\delta^{\circ}$ prism pl.
This experiment mass cuts
Barnham et al. mass cuts
t' (GeV^2)

fig.5

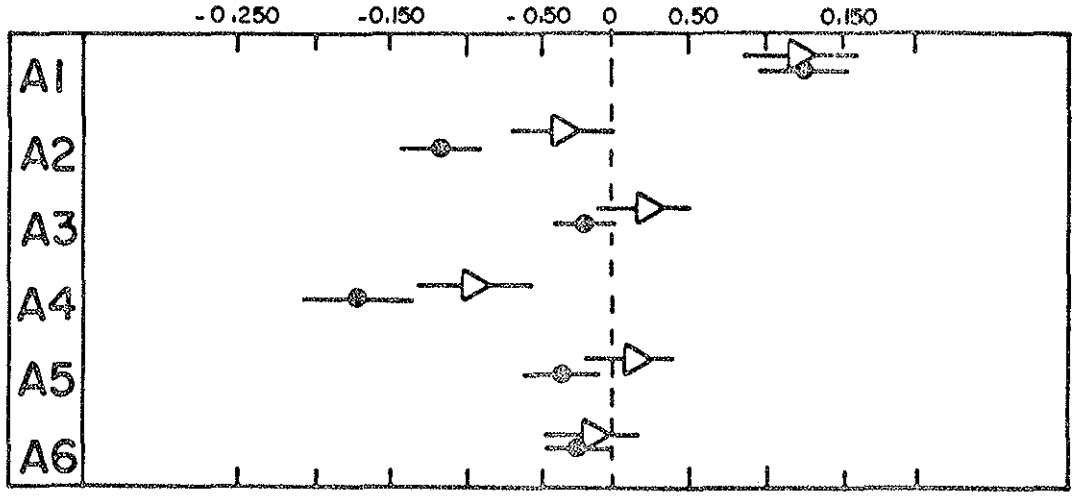

fig. 6

Prism plot selection

$\Delta^{\circ}\rho^{\circ}$ Box region for t' < .1